J. Math. Biology (1982) 15: 131 – 149

Journal of
Mathematical
Biology

Dynamics of Coupled Stomatal Oscillators

R. H. Rand[1], D. W. Storti[1], S. K. Upadhyaya[2], and J. R. Cooke[3]

[1] Department of Theoretical and Applied Mechanics, Cornell University, Ithaca, NY 14853, USA
[2] Department of Agricultural Engineering, University of Delaware, Newark, DE 19711, USA
[3] Department of Agricultural Engineering, Cornell University, Ithaca, NY 14853, USA

Abstract. Stomata are microscopic openings in the leaves of green plants which permit gas exchange. Stomata exhibit oscillatory opening and closing behavior under certain environmental conditions in addition to a daily (diurnal) cycle. In order to explore the effects of coupling between neighboring stomata we present a mathematical model of the dynamics of a system of N coupled stomatal oscillators. An individual stomate is modeled to either remain closed, oscillate periodically, or remain open, depending on the local water potential. Coupling between neighboring stomata is accomplished in the model by taking into account the flow of water in the leaf as well as by oscillator phase coupling.

Analysis of the model shows that under certain conditions it exhibits a stable spatially uniform synchronized behavior, referred to here as the in-phase mode. It is also shown that under non-uniform illumination the system may behave in a more complicated fashion.

Key words: Stomate – Oscillators – Dynamical systems

Introduction

CO_2 enters and water vapor exits the leaf interior through microscopic holes in the leaf surface called stomata. The stomatal apparatus consists of two specialized guard cells which surround the stomatal pore (Fig. 1). The pore size depends upon the changing hydrostatic (turgor) pressures in the guard cells and in the neighboring subsidiary cells [1]. In general, it is expected that the stomata will be open in the daylight, permitting CO_2 to enter the leaf where it is used in photosynthesis, but closed at night, preventing excessive water loss.

Although this general situation may be realistic in an average sense (i.e., for the behavior of a representative stomate, averaged over time and position), the behavior of a particular stomate can be more complicated [16]. In the first place, normal fluctuations in local light intensity, such as due to shading by clouds or by other leaves on the same plant, may produce stomatal closure during daylight hours. Moreover, even in *constant* environmental conditions stomata can *oscillate*, typically with a period of from 2 to 50 min [2], [3], [15], [20].

0303 – 6812/82/0015/0131/$03.80

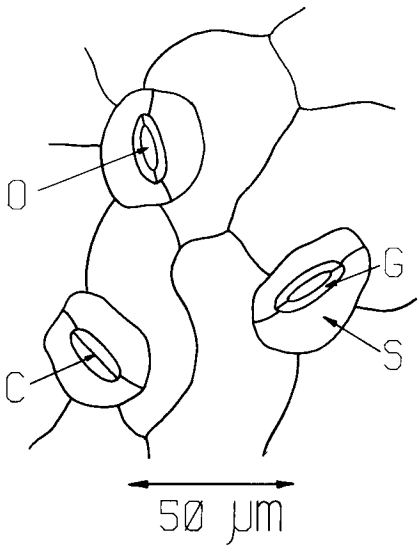

Fig. 1. View of the leaf surface showing stomatal pores in both open (O) and closed (C) states. G = guard cell, S = subsidiary cell

Thus even on the same leaf, some stomata may be open while others are closed. In particular this could result from the effects of dynamic interaction between neighboring stomata. That is, viewing each stomatal apparatus as a dynamical system, their individual behavior may be non-uniform due to the effects of *coupling*. In this fashion one may envision *waves* of stomatal opening moving across the leaf surface. Unfortunately experimental observations aimed at testing the existence of such phenomena are unavailable at the present time, although such studies are known to be in progress [17].

The purpose of the present paper is to investigate this subject by developing a mathematical model of the dynamics of coupled stomatal oscillators and analyzing its behavior. In doing so we realize that we are being somewhat conjectural. Nevertheless, we feel that this is an important use of mathematical models, i.e., to investigate the feasibility of a scientific idea prior to its experimental study, and we hope that this work will help to motivate plant physiologists to perform the associated experiments.

The Model

A. Simplified Stomatal Oscillator

We begin by reviewing previous research on mathematical models of stomatal oscillators. Delwiche and Cooke [3] proposed a model which was more recently analyzed by Rand et al. [4]. The model involved a system of two coupled ordinary differential equations and was based on conservation of water fluxes between guard cells, neighboring subsidiary cells and the rest of the plant. For a range of parameter values, the model exhibited a stable limit cycle oscillation [3]. The oscillation may be described briefly in words as follows: When the pore is open, water vapor exits from the leaf, lowering the hydrostatic pressure in the guard and subsidiary cells.

This eventually causes the pore to close, permitting the leaf vascular system to gradually replenish the water lost by the guard and subsidiary cells. This in turn raises the hydrostatic pressures in these cells and opens the pore.

The model in [3] was embedded in a one parameter family of models in [4], the parameter corresponding to the osmotic contents of the guard cell. As the parameter was tuned, a series of bifurcations was shown to occur, each resulting in a distinct dynamical behavior of the system. In particular, it was shown that as the parameter was increased, the steady state behavior of the pore went from i) an equilibrium state with closed pore, to ii) a periodic motion (a limit cycle) with sometimes open and sometimes closed pore, to iii) an equilibrium state with open pore.

In order to reduce the mathematical difficulties involved in considering N such oscillators with coupling, we propose the following simplified model of the dynamics of the stomatal apparatus. The model incorporates the most significant features of the complex dynamical behavior found in [4], while simplifying the original mathematical formulation of [3].

We postulate that the dynamical behavior of the pore width depends upon the water potential in the substomatal cavity, ψ, in the following manner: If $\psi \leqslant \psi_c$, the pore remains closed, while if $\psi \geqslant \psi_0$, the pore remains open, while if $\psi_c < \psi < \psi_0$, the pore oscillates, open for half the period and closed for the other half.

That is, let $F(\psi; t)$ be an indicator of the condition of the pore,

$$F = \begin{cases} 0, & \text{if the pore is closed,} \\ 1, & \text{if the pore is open.} \end{cases} \tag{1}$$

Then we assume (Fig. 2)

$$F(\psi; t) = \begin{cases} 0 & \psi \leqslant \psi_c \quad \text{(region I, closed),} \\ 1, & \psi \geqslant \psi_0 \quad \text{(region III, open),} \\ H(\sin\theta(t)), & \psi_c < \psi < \psi_0 \quad \text{(region II, oscillatory),} \end{cases} \tag{2}$$

where $\theta(t)$ is the phase of the stomatal oscillator, $H(\cdot)$ is the unit step function and where for brevity we refer to the intervals $\psi \leqslant \psi_c$, $\psi_c < \psi < \psi_0$ and $\psi \geqslant \psi_0$, respectively as regions I, II, and III.

Here we have assumed that the pore is either wide open or completely closed. Not only does this assumption simplify the analysis of the model, but it also agrees with results found earlier concerning gaseous diffusion through elliptical stomata.

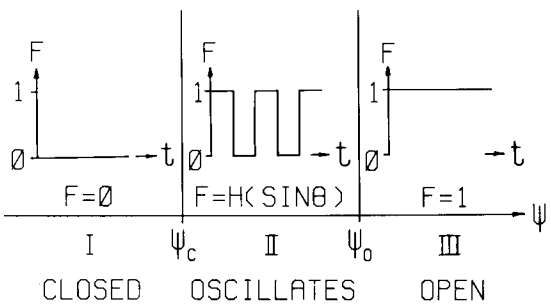

Fig. 2. Model of the dynamics of a single stomate. The pore condition indicator F depends upon the water potential in the substomatal cavity ψ. Trigger potentials ψ_c, ψ_0 are parameters

E.g. Cooke [5] showed that a slightly open stomate can permit relatively large diffusion rates. Thus, F represents the *effective* pore condition, taking into account gaseous fluxes through the pore rather than simply pore geometry.

We note that in [4] we varied a parameter which corresponded to the osmotic contents of the guard cell, while here we have considered the bifurcation parameter to be the water potential ψ. In fact, we have shown by an analysis similar to that in [4] that both these parameters have similar effects on the system dynamics. In any case we view the previous work [3], [4] as motivational, and we propose the present model of stomatal dynamics as independent from previous work and reasonable in its own right, as follows: Eqs. (1), (2) assume that when the leaf is sufficiently water stressed ($\psi \leqslant \psi_c$), a typical stomate remains closed, in qualitative agreement with experimental observations (see [15]). On the other hand, if water is sufficiently plentiful ($\psi \geqslant \psi_0$), then a typical stomate is assumed to remain open. This is in qualitative agreement with experimental observations in the case that other factors such as light intensity, CO_2 concentration or leaf temperature are not limiting [15]. For water potentials between these limits ($\psi_c < \psi < \psi_0$), the model assumes that a typical stomate oscillates. Here the experimentally observed state of oscillation is viewed as a kind of dynamical bridge between closed and open equilibrium states [4].

It remains to specify the phase $\theta(t)$. For a single stomate (uncoupled from its neighbors) we propose that the phase behave according to the equation

$$\frac{d\theta}{dt} = \omega \tag{3}$$

that is,

$$\theta = \omega(t - t_0) + \theta_0 \tag{4}$$

where ω = frequency of stomatal oscillator, t_0 = time at which system most recently entered the oscillatory state (region II), θ_0 = the initial phase at time t_0.

We select the initial phase θ_0 that the system is given at the beginning of its oscillation so as to insure maximum continuity with respect to its previous equilibrium state. Thus, e.g., if the system enters region II from region I (closed pore), we take θ_0 to be π radians, whereupon the pore stays closed for half a period. We assume

$$\theta_0 = \begin{cases} \pi, & \text{if most recent entry into region II was from region I,} \\ 0, & \text{if most recent entry into region II was from region III.} \end{cases} \tag{5}$$

This completes the description of the dynamical stomatal element which gives effective pore condition F as a function of ψ. In order to utilize this element in a model of coupled stomatal oscillators we next consider the flow of water in the leaf.

B. Flow of Water in the Leaf

Water enters the leaf through the petiole xylem tissue and follows a branching network of vascular conduits of decreasing diameter. This continues until the flowing water reaches the xylem termini which are distributed ubiquitously

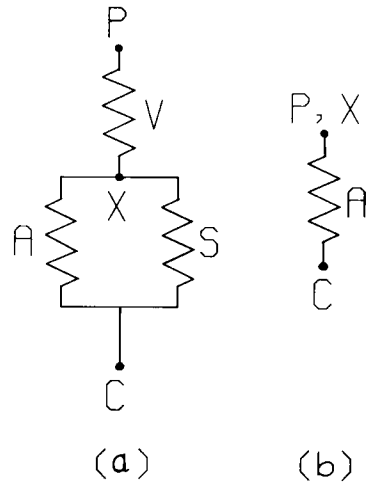

Fig. 3. Resistances to water flow in the leaf. P = petiole, V = vascular conduits, X = xylem terminal, A = mesophyll apoplasm, S = mesophyll symplasm, C = substomatal cavity. If we neglect potential drops in the vascular conduits and flow in the symplasm, we may replace Fig. 3a by 3b

throughout the leaf. From the xylem termini the water proceeds mainly through the cell wall apoplasm of the leaf mesophyll to the substomatal cavities, and then, if the stomatal pore is open, to the leaf exterior in the form of water vapor.

In this work we shall neglect the drops in water potential which occur in the vascular conduits from the petiole to the xylem termini as compared to the drops in water potential encountered in the mesophyll apoplasm between the xylem termini and the substomatal cavities ([18], p. 394). We shall also neglect flow in the mesophyll symplasm as compared to flow in the apoplasm ([19], p. 51). That is, we assume (Fig. 3a)

$$R_{\text{conduits}} \ll R_{\text{apoplasm}} \ll R_{\text{symplasm}}, \tag{6}$$

where each R is the resistance to water flow in the appropriate region. With these assumptions, we are effectively replacing Fig. 3a by Fig. 3b.

In order to obtain the equations governing the coupling between neighboring stomata, we will balance water fluxes in the apoplasm of the mesophyll cells. For simplicity we consider a one dimensional arrangement of N stomata in a straight line (Fig. 4).

Taking a control volume consisting of the cell walls in all mesophyll cells lying in the neighborhood of a given stomate, the rate of accumulation of water volume in the control volume is

$$V\frac{dn}{dt}, \tag{7}$$

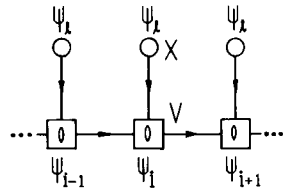

Fig. 4. Water fluxes in a one dimensional arrangement of stomata. X = xylem termini, V = control volume of mesophyll cell walls in the neighborhood of a stomate

where V = control volume (cm^3), n = volumetric water content of the control volume (cm^3/cm^3).

Following Molz [6] we assume

$$\frac{dn}{dt} = S\frac{d\psi}{dt}, \tag{8}$$

where S = storage coefficient for the cell wall (bar^{-1}), ψ = representative water potential in the control volume (bar). For simplicity, we assume in Eq. (8) that

$$\psi = \psi_i, \tag{9}$$

where ψ_i = water potential in cell wall apoplasm of the ith substomatal cavity (bar).

We balance expression (7) with the net rate of flow into the control volume. We include three terms (Fig. 4):

i) Flux from the xylem terminal to the ith stomate:

$$\frac{aP}{L}(\psi_l - \psi_i), \tag{10}$$

where a = area of apoplasm pathway perpendicular to flow direction (cm^2), P = hydraulic conductivity of cell wall material (cm^2/sec bar), L = distance between xylem terminal and substomatal cavity (cm), ψ_l = water potential at a xylem terminal, assumed the same for all i, since we neglect water potential drops in the vascular conduits (bar).

ii) Flux between ith stomate and neighboring stomata:

$$\frac{aP}{d}(\psi_{i+1} - 2\psi_i + \psi_{i-1}), \tag{11}$$

where d = distance between neighboring stomata (cm).

iii) Flux out the ith stomatal pore, if it is open:

$$-a_{st}JF, \tag{12}$$

where J = flux of water from the apoplasm cell walls of the substomatal cavity to the vapor phase, taken per unit leaf surface area (cm^3/cm^2 sec), a_{st} = effective leaf area corresponding to a single pore (cm^2) = d^2, and where F indicates the pore condition (Eq. (1)).

Balancing expression (7) with expressions (10)–(12), using Eqs. (8), (9), and taking ψ_l to be independent of time t, we obtain:

$$k_1\frac{d\psi_i}{dt} = k_2(\psi_{i+1} - 2\psi_i + \psi_{i-1}) + k_3(\psi_l - \psi_i) - k_4F(\psi_i; t), \quad i = 1, 2, \ldots, N, \tag{13}$$

where $k_1 = VS$, $k_2 = aP/d$, $k_3 = aP/L$, $k_4 = a_{st}J$, and where we take $\psi_0 = \psi_1$ and $\psi_{N+1} = \psi_N$ to be dummy variables invoked to permit Eq. (13) to be valid for $i = 1$ and N, respectively.

C. Phase Coupling

Through the water potential coupling of Eq. (13), the state of the ith stomate may be influenced by the water potential of its neighbors. Specifically, the ith stomate may be moved from a given region (I, II or III, cf. Fig. 2) to another region by this type of coupling.

However, if a group of neighboring stomata are all in region II, then from Eq. (2) their respective pore conditions (i.e., open or closed) depend only on their phases $\theta_i(t)$ and not on their water potentials $\psi_i(t)$. Since the phase $\theta_i(t)$ is determined either from the initial condition $\theta_i(0)$ or from the instant of time at which the ith stomatal oscillator enters region II, Eq. (13) provides no possibility of "phase diffusion" (or "phase-coupling").

Now recent studies of systems of coupled limit cycle oscillators (e.g., [7]–[10]) shows that such systems generally exhibit phase coupling. The physical basis for phase coupling in our model resides in the influence which effective pore condition has on local water potential. When the pore of an oscillating stomate closes, water which had been flowing from the xylem termini to the leaf exterior through the open pore is now available for redistribution to neighboring stomata. This causes a change in local water potential and an accompanying change in local water flow patterns which could cause a neighboring stomate to close sooner or later than it would have if no coupling were present, thereby changing its phase.

We can introduce phase coupling into our model by modifying Eq. (3) as follows:

$$\frac{d\theta_i}{dt} = \omega + \text{coupling terms}. \tag{14}$$

The question of how to choose the coupling terms may be answered by referring to other work on similar systems [7]–[10].

Winfree ([10], p. 125) suggests the diffusive expression

$$\text{coupling terms} = k(\theta_{i+1} - \theta_i) + k(\theta_{i-1} - \theta_i),$$

where k is a coupling constant. However, since θ_i is defined on S^1, this expression must be interpreted mod 2π. An alternative would be to take

$$\text{coupling terms} = kf(\theta_{i+1} - \theta_i) + kf(\theta_{i-1} - \theta_i),$$

where $f(\cdot)$ is a 2π-periodic function. This course was taken by Cohen, et al. [8], where f was taken as the sine function. The resulting system (14) was studied in [8] and was shown to generate stable "phase locked" motions if the coupling was strong enough. This result agreed with the more realistic model of two strongly coupled van der Pol oscillators studied in [7].

In order to describe the phase coupling of stomatal oscillators in region II, we shall adopt the approach of [8], and write

$$\text{region II:} \quad \frac{d\theta_i}{dt} = \omega + k_5[\sin(\theta_{i+1} - \theta_i) + \sin(\theta_{i-1} - \theta_i)], \quad i = 1, 2, \ldots, N, \tag{15}$$

where k_5 is a coupling coefficient. Here we have assumed that each of the oscillators has the same uncoupled frequency ω and the same coupling coefficient k_5. As in Eq.

(13) we take $\theta_0 = \theta_1$ and $\theta_{N+1} = \theta_N$ to be dummy variables in region II invoked to permit Eq. (15) to be valid for $i = 1$ and N, respectively.

In order to conveniently adjust the initial phase of θ_i in accordance with Eq. (5), we associate values of θ_i with all stomata, even those in regions I and III which do not oscillate:

$$\text{region I:} \quad \theta_i = \pi, \tag{16}$$

$$\text{region III:} \quad \theta_i = 0. \tag{17}$$

This implies, e.g., that when a stomate enters region II from region I, its phase is initially set to π, by continuity of $\theta_i(t)$.

Non-Dimensionalization

The model of coupled stomatal oscillators derived above is contained in Eqs. (13), (2) and (15)–(17). In order to simplify the handling of these equations, we define the non-dimensional variables

$$u_i = \frac{\psi_i - \psi_c}{\psi_0 - \psi_c}, \tag{18}$$

$$\tau = \frac{k_3}{k_1} t. \tag{19}$$

Upon substitution these give for $i = 1, 2, \ldots, N$,

$$\frac{du_i}{d\tau} = C(u_{i+1} - 2u_i + u_{i-1}) + A - u_i - BF(u_i; \tau), \tag{20}$$

$$F(u_i; \tau) = \begin{cases} 0, & u_i \leqslant u_{ci} \quad \text{(region I)}, \\ 1, & u_i \geqslant u_{0i} \quad \text{(region III)}, \\ H(\sin\theta_i(\tau)), & u_{ci} < u_i < u_{0i} \quad \text{(region II)}, \end{cases} \tag{21}$$

$$\text{region II:} \quad \frac{d\theta_i}{d\tau} = \gamma + \mu[\sin(\theta_{i+1} - \theta_i) + \sin(\theta_{i-1} - \theta_i)], \tag{22}$$

$$\text{region I:} \quad \theta_i = \pi, \tag{23}$$

$$\text{region III:} \quad \theta_i = 0, \tag{24}$$

where

$$A = \frac{\psi_l - \psi_c}{\psi_0 - \psi_c}, \tag{25}$$

$$B = \frac{k_4}{k_3(\psi_0 - \psi_c)}, \tag{26}$$

$$C = \frac{k_2}{k_3}, \tag{27}$$

$$u_{ci} = \frac{\psi_{ci} - \psi_c}{\psi_0 - \psi_c}, \tag{28}$$

$$u_{0i} = \frac{\psi_{0i} - \psi_c}{\psi_0 - \psi_c}, \tag{29}$$

$$\gamma = \frac{\omega k_1}{k_3}, \tag{30}$$

$$\mu = \frac{k_1 k_5}{k_3}. \tag{31}$$

Note that although the non-dimensional water potential u_i is defined in Eq. (18) with respect to particular constants, ψ_c, ψ_0, each stomatal oscillator is permitted to have its own trigger potentials, ψ_{ci}, ψ_{0i}, respectively producing the non-dimensional parameters u_{ci}, u_{0i} in Eqs. (21), (28), and (29). This will be of importance in the case of a non-uniformly illuminated leaf, to be discussed later.

Parameter Estimation

The following parameter estimates are intended to give order of magnitude approximations but are not meant to represent statistical averages.

Flux parameters. Molz [6] estimates the storage coefficient S to lie between 0.03 and 0.07 bar^{-1}. We will take

$$S = 0.05\,\text{bar}^{-1}.$$

Molz [6] also gives the following estimate for hydraulic conductivity P:

$$P = 2.1 \times 10^{-7}\,\text{cm}^2/\text{sec bar}.$$

Cooke and Rand [11] estimate the evaporative flux J to be

$$J = 6.2 \times 10^{-6}\,\text{cm}^3/\text{cm}^2\,\text{sec}.$$

Geometrical Parameters. Meidner and Mansfield [12] give a wide range of values for stomatal density, with an average value of 140 stomata per mm^2 of leaf surface. This corresponds to a distance between neighboring stomata of 84 μm.

Philpott [13] gives an average maximum distance separating the smallest veins in *Ficus* as 155 μm, which we understand to represent the distance between neighboring xylem termini.

Based on these values we will take the parameters L and d to be approximated by the representative length of 100 μm:

$$L = d = 10^{-2}\,\text{cm}, \qquad a_{st} = d^2 = 10^{-4}\,\text{cm}.$$

To estimate the parameter a we assume the apoplasm (cell wall) pathway to have a cross-section 50 μm wide by 50 μm deep, and to be densely packed by cubical cells 10 μm on a side, each with cell walls which are 1 μm thick. The pathway cross-section then consists of 25 such cells, each cell having a cell wall cross-section of about 40 μm^2. This gives

$$a = 10^{-5}\,\text{cm}^2.$$

To estimate the parameter V we assume the control volume to consist of a cubical region 100 μm on a side, densely packed with cubical cells as above. Then

there are 1000 cells in the control volume and each has a cell wall volume of about 600 μm^3. This gives

$$V = 6 \times 10^{-7}\,\text{cm}^3.$$

Dynamical Parameters. Barrs [2] gives the period of hydraulically induced stomatal oscillations as ranging from 10 to 50 minutes. We take a representative period of 20 minutes, giving

$$\omega = 5.2 \times 10^{-3}\,\text{sec}^{-1}.$$

We performed numerical experiments on the Delwiche and Cooke model [3] which suggest that $\psi_0 - \psi_c$ is on the order of several bars. We take

$$\psi_0 - \psi_c = 3\,\text{bars}.$$

Substitution of the above estimates into the parameters k_i appearing in Eq. (13) yields:

$$k_1 = VS = 3 \times 10^{-8}\,\text{cm}^3\,\text{bar}^{-1},$$
$$k_2 = aP/d = 2.1 \times 10^{-10}\,\text{cm}^3\,\text{bar}^{-1}\,\text{sec}^{-1},$$
$$k_3 = aP/L = 2.1 \times 10^{-10}\,\text{cm}^3\,\text{bar}^{-1}\,\text{sec}^{-1},$$
$$k_4 = a_{st}J = 6.2 \times 10^{-10}\,\text{cm}^3/\text{sec}.$$

These values give the following non-dimensional parameters:

$$B = \frac{k_4}{k_3(\psi_0 - \psi_c)} = 0.98,$$
$$C = k_2/k_3 = 1,$$
$$\gamma = \omega k_1/k_3 = 0.74.$$

The In-Phase Mode

Although Eqs. (20) – (24) are too difficult to solve analytically in general, we can obtain an exact solution in the special case of N identical oscillators executing the in-phase mode:

$$u(\tau) = u_1(\tau) = u_2(\tau) = \cdots = u_N(\tau). \tag{32}$$

This motion is particularly important since it represents synchronized behavior and will be shown to be the steady state behavior of the system for a wide range of parameter values.

The in-phase mode satisfies the equations:

$$\frac{du}{d\tau} = A - u - BF(u;\tau), \tag{33}$$

$$F(u;\tau) = \begin{cases} 0, & u \leqslant 0 \quad \text{(region I)}, \\ 1, & u \geqslant 1 \quad \text{(region III)}, \\ H(\sin\theta(\tau)), & 0 < u < 1 \quad \text{(region II)}, \end{cases} \tag{34}$$

$$\theta = \gamma(\tau - \tau_0) + \theta_0, \tag{35}$$

where θ_0 is given by Eq. (5).

The behavior of the in-phase mode depends upon the parameters A, B, and γ. We fix B and γ, and vary A. The parameter A represents the availability of water at the xylem termini.

For $A \leqslant 0$ the in-phase mode is an equilibrium at $u = A \leqslant 0$ (in region I), while for $A \geqslant 1 + B$ it is an equilibrium at $u = A - B \geqslant 1$ (in region III).

For $0 < A < 1 + B$ the in-phase mode is a periodic motion which may be described by four parameters:

u_L = minimum value of u occurring during the periodic motion,

u_R = maximum value of u occurring during the periodic motion,

T_c = the portion of the oscillation period during which the pore is closed and u is increasing,

T_0 = the portion of the oscillation period during which the pore is open and u is decreasing.

These parameters are subject to the constraints that the motion must remain in region II and that u cannot increase (or decrease) for more than half of the natural period (the period equals $2\pi/\gamma$):

$$u_L \geqslant 0, \tag{36}$$

$$u_R \leqslant 1, \tag{37}$$

$$T_c \leqslant \pi/\gamma, \tag{38}$$

$$T_0 \leqslant \pi/\gamma. \tag{39}$$

In order to find these parameters analytically for given A, B, and γ we proceed as follows:

When the pore is closed, Eq. (33) becomes

$$\frac{du}{d\tau} = A - u \tag{40}$$

which has the general solution

$$u(\tau) = A + [u(0) - A]e^{-\tau}. \tag{41}$$

For the periodic motion we take $u(0) = u_L$, $\tau = T_c$, and $u(\tau) = u_R$:

$$u_R = A + (u_L - A)e^{-T_c}. \tag{42}$$

When the pore is open, Eq. (33) becomes

$$\frac{du}{d\tau} = A - u - B \tag{43}$$

which has the general solution

$$u(\tau) = A - B + [u(0) - A + B]e^{-\tau}. \tag{44}$$

For the periodic motion we take $u(0) = u_R$, $\tau = T_0$, and $u(\tau) = u_L$:

$$u_L = A - B + (u_R - A + B)e^{-T_0}. \tag{45}$$

Although Eqs. (42) and (45) are two equations for four unknowns, it turns out that due to the constraints (36)–(39), a unique solution exists. The motion with u increasing will cease either because $u_R = 1$ or $T_c = \pi/\gamma$, whichever comes first, while the motion with u decreasing will cease either because $u_L = 0$ or $T_0 = \pi/\gamma$.

There are four cases, depending on which constraints apply:

Case i) $T_c = \pi/\gamma, \quad T_0 = \pi/\gamma.$ (46)

Case ii) $T_c = \pi/\gamma, \quad u_L = 0.$ (47)

Case iii) $u_R = 1, \quad T_0 = \pi/\gamma.$ (48)

Case iv) $u_R = 1, \quad u_L = 0.$ (49)

In each case substitution of the appropriate pair of constraints (46)–(49) into Eqs. (42) and (45) specifies the other two parameters. We find:

Case i)
$$u_R = A - \frac{B}{1 + e^{\pi/\gamma}}, \tag{50}$$

$$u_L = A - \frac{B}{1 + e^{-\pi/\gamma}}. \tag{51}$$

Case ii)
$$u_R = A(1 - e^{-\pi/\gamma}), \tag{52}$$

$$T_0 = \ln\left[\frac{B - Ae^{-\pi/\gamma}}{B - A}\right]. \tag{53}$$

Case iii)
$$T_c = \ln\left[\frac{(1 - A + B)e^{-\pi/\gamma} - B}{1 - A}\right], \tag{54}$$

$$u_L = (1 - A + B)e^{-\pi/\gamma} + A - B. \tag{55}$$

Case iv)
$$T_c = \ln\left[\frac{A}{A - 1}\right], \tag{56}$$

$$T_0 = \ln\left[\frac{1 + B - A}{B - A}\right]. \tag{57}$$

For a given set of parameters, A, B, γ, evidently only one case is possible. To find the parameters characterizing the periodic motion, substitute A, B, γ into Eqs. (50)–(57) and eliminate those cases which give parameter values which violate the constraints (36)–(39).

E.g. for $A = 1$, $B = 0.98$, $\gamma = 0.74$, we find that $\pi/\gamma = 4.24$ and

Case i) $u_R = 0.986$, OK,

$u_L = 0.034$, OK.

Case ii) $u_R = 0.986$, OK,

$T_0 =$ complex, REJECT.

Case iii) $T_c =$ infinite, REJECT,

$u_L = 0.034$, OK.

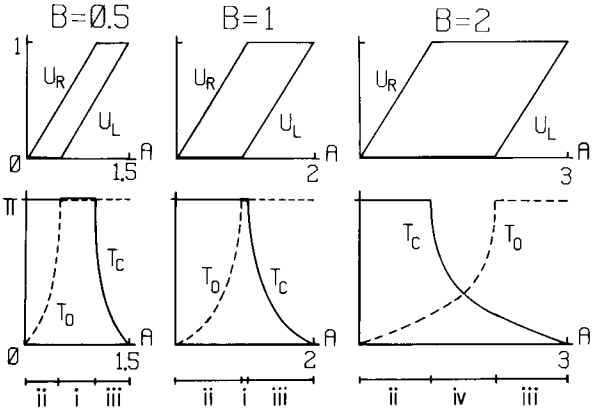

Fig. 5. Parameters describing the in-phase periodic motion for $\gamma = 1$ and for $B = 0.5, 1, 2$. The parameter A varies from 0 to $1 + B$. The associated case number (i–iv) is shown at the bottom of the figure

Case iv) T_c = infinite, REJECT,

T_0 = complex, REJECT.

Note that only case i) does not violate the constraints (36)–(39). Thus for this example, we conclude that the periodic motion is described by the following parameter values:

$$u_L = 0.034, \qquad u_R = 0.986, \qquad T_c = T_0 = 4.24.$$

In this fashion we may generate the parameters describing the periodic motion for fixed B, γ while A varies from 0 to $1 + B$ (see Fig. 5). Notice that as A increases from a value less than 0 to a value larger than $1 + B$, the fraction of time during which the pore is open ($T_0/(T_0 + T_c)$) *gradually* increases from zero to unity. Thus, while the stomatal element itself (Eq. (2)) is defined so as to change *abruptly* from one region to another with a change in water potential, ψ, the whole system (i.e., the stomatal element plus its water supply, Eqs. (2), (13)), when executing the in-phase mode, responds in a continuous fashion to a change in leaf water potential, ψ_l.

Numerical Results and Stability

In order to further understand the behavior of the model we numerically integrated the governing Eqs. (20)–(24) using finite differences. Typical results are displayed in Figs. 6, 7, for which $A = 3$, $B = 1$, $C = 1$, $\gamma = 1$, $\mu = 1$, $N = 20$. Fig. 6 shows dimensionless water potential u and phase θ as functions of position for various times τ. Note that while the initial conditions were chosen so that equal portions of the leaf were in each of the regions I, II, III, the system quickly approached the in-phase mode, which in this case is an equilibrium state in region III with $u = A - B = 2$, $\theta = 0$. Fig. 7 is a plot of time versus position showing which stomata lie in each of the regions I, II, III.

Note from Figs. 6 and 7 that the in-phase mode is evidently asymptotically stable. This can be shown analytically by setting

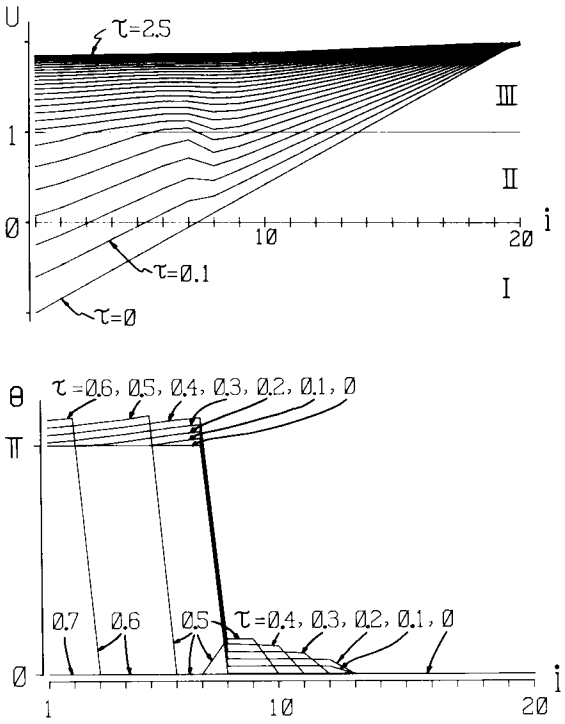

Fig. 6. Results of numerical integration of Eqs. (20)–(24) for $A = 3$, $B = 1$, $C = 1$, $\gamma = 1$, $\mu = 1$, $N = 20$. The initial conditions on u are as shown. The initial conditions on θ are zero for those elements initially in region II

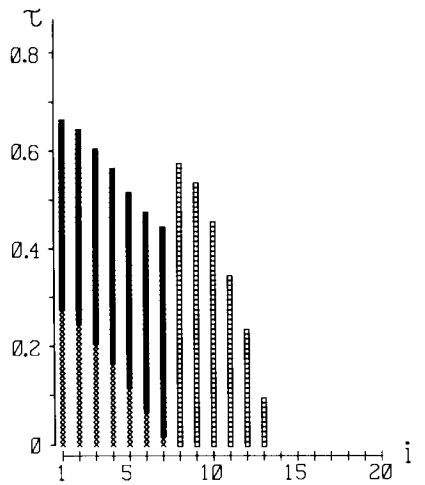

Fig. 7. Results of numerical integration, same data as Fig. 6. Here and in Figs. 8, 10 an × means pore closed, a blank means pore open and a box means region II. That is, × = region I (*pore closed*), ⊠ = region II (*pore closed*), □ = region II (*pore open*), and a blank = region III (*pore open*)

$$u_i(\tau) = u^* + \xi_i(\tau), \qquad i = 1, 2, \ldots, N, \tag{58}$$

where u^* = equilibrium value of the in-phase mode, $\xi_i(\tau)$ = small deviation from the steady state in-phase mode. The equilibrium state $u_i(\tau) = u^*$ will be said to be asymptotically stable if $\xi_i(\tau) \to 0$ as $\tau \to \infty$ for all (arbitrarily small) initial conditions, $\xi_i(0)$.

Substituting (58) into (20) and using (33) gives

$$\frac{d\xi_i}{d\tau} = C(\xi_{i+1} - 2\xi_i + \xi_{i-1}) - \xi_i - B\,\delta F_i, \tag{59}$$

where

$$\delta F_i = F(u^* + \xi_i; \tau) - F(u^*; \tau). \tag{60}$$

Since $F(u^*; \tau)$ is a constant (equal to either 0 or 1), then for sufficiently small deviations ξ_i, $F(u^* + \xi_i; \tau)$ is the same constant, and so δF_i vanishes in (59):

$$\frac{d\xi_i}{d\tau} = C(\xi_{i+1} - 2\xi_i + \xi_{i-1}) - \xi_i, \qquad i = 1, 2, \ldots, N. \tag{61}$$

We want the general solution to (61) subject to the boundary conditions

$$\xi_0 = \xi_1 \qquad \text{and} \qquad \xi_{N+1} = \xi_N \tag{62}$$

which are invoked in order to permit Eq. (61) to be valid for $i = 1$ and N, respectively.

We assume a solution in the form [14]

$$\xi_i(\tau) = e^{\lambda\tau}\cos(\Omega i + \beta), \qquad i = 1, 2, \ldots, N, \tag{63}$$

where λ, Ω and β are unknown constants. Substituting (63) into (61) and equating coefficients of $\cos(\Omega i + \beta)$ gives

$$\lambda = -1 - 2C(1 - \cos\Omega), \tag{64}$$

where we have used the identity

$$\cos[\Omega(i+1) + \beta] + \cos[\Omega(i-1) + \beta] = 2\cos\Omega\cos(\Omega i + \beta).$$

Substituting (63) into the boundary condition (62) gives

$$\cos\beta = \cos(\Omega + \beta) \tag{65}$$

and

$$\cos[\Omega(N+1) + \beta] = \cos(\Omega N + \beta). \tag{66}$$

Eqs. (65), (66) may be rewritten using the usual trigonometric identities as

$$\tan\beta = \frac{-1 + \cos\Omega}{\sin\Omega} = \frac{-1 + \cos\Omega - \sin\Omega\tan N\Omega}{\sin\Omega + (-1 + \cos\Omega)\tan N\Omega}. \tag{67}$$

Eq. (67) is satisfied by taking

$$\tan N\Omega = 0, \tag{68}$$

that is,

$$\Omega = \frac{k\pi}{N}, \qquad k = 0, 1, \ldots, N-1. \tag{69}$$

When the N values of Ω in Eq. (69) and the corresponding values of λ and β from Eqs. (64) and (67) are substituted into Eq. (63), we obtain N linearly independent solution vectors $\xi_i(\tau)$ which span the solution space of Eq. (61). From (64) we see that for $C \geqslant 0$ (Eq. (27)), the eigenvalue $\lambda \leqslant -1 < 0$ for each $k = 0, 1, \ldots, N-1$

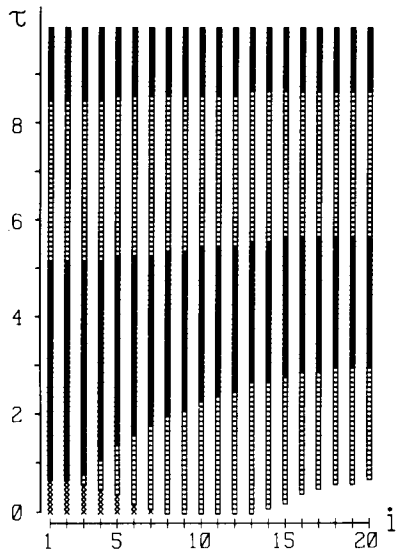

Fig. 8. Results of numerical integration for $A = 1$, $B = 1$, $C = 1$, $\gamma = 1$, $\mu = 15$, $N = 20$. See caption of Fig. 7 for meaning of symbols. Initial conditions are as in Fig. 6

and hence $\xi_i(\tau) \to 0$ as $\tau \to \infty$ for all initial conditions $\xi_i(0)$, yielding the result that the equilibrium in-phase motions are asymptotically stable for $C \geqslant 0$.

The question of the stability of the periodic in-phase motions turns out to be more difficult. Specifically, the linearized variational equations corresponding to Eq. (22) for the phases $\theta_i(\tau)$ can be shown to have a zero eigenvalue, indicating that a non-linear stability analysis is required.

Nevertheless we may obtain stability information by numerical integration. E.g., consider Fig. 8 for which $A = 1, B = 1, C = 1, \gamma = 1, \mu = 15, N = 20$. After a brief transient period associated with the initial conditions, the system rapidly approached the case i) periodic in-phase motion (cf. Fig. 5). Similarly we found the periodic in-phase motion to be stable for all other parameter values for which we ran numerical experiments, except for $\mu = 0$. In the absence of phase coupling ($\mu = 0$) the model lacks any mechanism for synchronization of neighboring oscillators and instability of the periodic in-phase motion is expected and observed.

By varying the model parameters one at a time, we were able to find the following trends: increasing the water potential diffusion coefficient C decreases the time it takes for an oscillator to enter the region in which it will finally remain, but it does not strongly influence the time for the system to become phase-locked once it is entirely in region II, in the case of a periodic in-phase motion (Fig. 8). An increase in the phase diffusion coefficient μ, on the other hand, speeds up the latter effect without strongly influencing the former. An increase in the number of oscillators N tends to retard the system's approach to steady state and is qualitatively equivalent to decreasing both C and μ. An increase in γ reduces the dimensionless period of the stomatal oscillations in region II.

Non-Uniform Illumination

It has been observed experimentally that an increase in illumination, I, tends to open the stomatal pore [15]. (Here we assume that other factors such as water

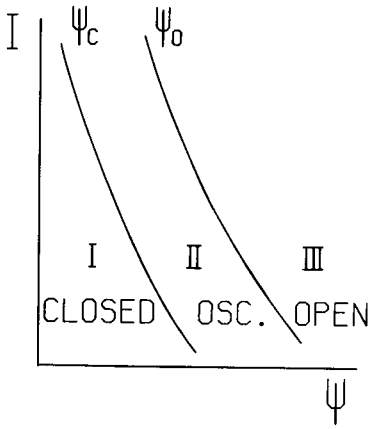

Fig. 9. For a given illumination I the trigger potentials ψ_c, ψ_0 determine the regions I, II, III which define the behavior of a single stomatal oscillator (Fig. 2). We require ψ_c and ψ_0 to decrease with increases in I in order that the pore tend to open with an increase in illumination

stress, atmospheric CO_2 concentration, or temperature do not supersede the effects of illumination and cause the pore to close.)

In order to include the effects of variable illumination in the model we will take the trigger potentials ψ_c and ψ_0 (cf. Eq. (2)) to depend on I as in Fig. 9.

As an example, suppose half the stomata ($i = 1, 2, \ldots, N/2$) are illuminated while the other half are not. Let ψ_c, ψ_0 and $\psi_c + v$, $\psi_0 + v$ respectively represent the illuminated and unilluminated trigger potentials. Then Eqs. (28), (29) give

ILLUMINATED	$\psi_{ci} = \psi_c$,	$u_{ci} = 0$,
$i = 1, 2, \ldots, N/2$	$\psi_{0i} = \psi_0$,	$u_{0i} = 1$,
UNILLUMINATED	$\psi_{ci} = \psi_c + v$,	$u_{ci} = v/(\psi_0 - \psi_c)$,
$i = (N/2) + 1, \ldots, N$	$\psi_{0i} = \psi_0 + v$,	$u_{0i} = 1 + v/(\psi_0 - \psi_c)$.

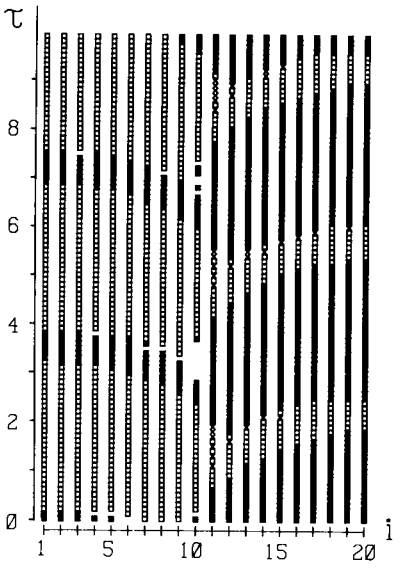

Fig. 10. Results of numerical integration for a non-uniformly illuminated leaf with $A = 1.5$, $B = 1$, $C = 1$, $\gamma = 1$, $\mu = 5$, $v = \psi_0 - \psi_c$, $N = 20$. Here stomata $1-10$ are illuminated and $11-20$ are unilluminated. Exhibited data represents steady state behavior. See caption of Fig. 7 for meaning of symbols

By varying $\nu/(\psi_0 - \psi_c)$ and A for fixed B, C, γ, μ we found by numerical integration that it is possible to produce stomatal opening in the illuminated half of the leaf while the unilluminated half remains closed. We were also able to simulate cases where stomata in half the leaf were in equilibrium while those in the other half were oscillating.

More interesting, however, is the case in which both halves oscillate but with different open and closed times T_0, T_c. Consider, e.g., Fig. 10, for which $A = 1.5$, $B = C = \gamma = 1, \mu = 5, \nu = \psi_0 - \psi_c, N = 20$. The in-phase mode for the illuminated half has $T_0 = 3.14$, $T_c = 0.67$ (Fig. 5), while for the unilluminated half it turns out that $T_0 = 0.67$, $T_c = 3.14$. Note that oscillators numbers 10 and 11 behave more irregularly than the others. These are located closest to the transition between illuminated and unilluminated regions. Oscillators numbers 1, 2 and 19, 20, on the other hand, are relatively uninfluenced by the non-uniform illumination and behave as they would in a uniform situation. Oscillators numbers $3-9$ and $12-18$ exhibit steady state phase lags while maintaining relatively regular behavior.

Figure 10 demonstrates that the model can exhibit complicated dynamical behavior in the presence of spatially non-uniform but time independent illumination loading. It is clear that by permitting the illumination to vary in time as well, the system dynamics can become even more diverse.

Conclusions

We have shown that the model exhibits a stable, spatially uniform, synchronous motion, the in-phase mode. If a real leaf were to behave the way our model does in this mode, then examination of any single stomate would indicate the state of the entire population of leaf stomata. Indeed this behavior is assumed (usually implicitly) in experiments which measure the behavior of some related average quantity. For in order to conclude, e.g., that an oscillation in the CO_2 concentration in a chamber containing a leaf reflects an oscillation in the behavior of the stomata, it is necessary to assume that all the stomata are behaving in a similar fashion.

On the other hand our model also exhibits transients associated with a sudden change in parameters (e.g. illumination level or water potential). From Eqs. (20) or (64), (69) we can estimate the transient time to be about one dimensionless time unit, a value that agrees with the numerical simulations in Figs. $6-8$, being approximately the time for the initial transients to disappear. Using Eq. (19), this estimate corresponds to about k_1/k_3 sec., or using the parameter estimates given in this paper, about 140 sec.

Application of this result to a real leaf would suggest the following caveat to experimenters using devices which inadvertently involve initiation of transients: If the time required for the attachment and use of the instrument is of the order of a minute, then the leaf probably has enough time to significantly change its dynamical state. Thus the measurement may reflect the presence of the experimental equipment to a greater extent than is desirable. This would apply, e.g., to the porometer, a cup-like device which is clamped onto part of a leaf, permitted to come to gaseous equilibrium with the leaf surface and then analyzed for the water vapor content of the air inside the cup.

Moreover we note that the model exhibits spatially nonuniform behavior in response to nonuniform illumination loading. Thus if an experimental device is attached to only part of a leaf, it may alter the dynamical state of the stomata near it and once again give rise to spurious results.

In closing we wish to state that we see this work as representing only a first step in the study of stomatal oscillation fields. Nevertheless we feel that we have shown that the subject of leaf dynamics is considerably more complicated than previous treatments have indicated.

Acknowledgement. The authors wish to thank Professor Tim Setter of Cornell University for helpful discussions.

References

1. Cooke, J. R., DeBaerdemaeker, J. G., Rand, R. H., Mang, H. A.: A finite element shell analysis of guard cell deformations. Trans. ASAE **19**, 1107–1121 (1976)
2. Barrs, H. D.: Cyclic variations in stomatal aperture, transpiration, and leaf water potential under constant environmental conditions. Ann. Rev. Plant Physiol. **22**, 223–236 (1971)
3. Delwiche, M. J., Cooke, J. R.: An analytical model of the hydraulic aspects of stomatal dynamics. J. Theoret. Biology **69**, 113–141 (1977)
4. Rand, R. H., Upadhyaya, S. K., Cooke, J. R., Storti, D. W.: Hopf bifurcation in a stomatal oscillator. J. Math. Biol. **12**, 1–11 (1981)
5. Cooke, J. R.: Some theoretical considerations in stomatal diffusion: A field theory approach. Acta Biotheoretica **17**, 95–124 (1967)
6. Molz, F. J.: Water transport through plant tissue: The apoplasm and symplasm pathways. J. Theor. Biol. **59**, 277–292 (1976)
7. Storti, D. W., Rand, R. H.: Dynamics of two strongly coupled van der Pol oscillators. Int. J. Nonlinear Mechanics, in press (1982)
8. Cohen, A. H., Holmes, P. J., Rand, R. H.: The nature of the coupling between segmental oscillators of the lamprey spinal generator for locomotion: A mathematical model. J. Math. Biol. **13**, 345–369 (1982)
9. Rand, R. H., Holmes, P. J.: Bifurcation of periodic motions in two weakly coupled van der Pol oscillators. Int. J. Nonlinear Mechanics **15**, 387–399 (1980)
10. Winfree, A. T.: The geometry of biological time, pp. 530. Berlin-Heidelberg-New York: Springer 1980
11. Cooke, J. R., Rand, R. H.: Diffusion resistance models. In: Predicting photosynthesis for ecosystem models (Hesketh, J. D., Jones, J. W., eds.) Vol. 1, pp. 93–121. Boca Raton, Fla: CRC Press 1980
12. Meidner, H., Mansfield, T. A.: Physiology of stomata, pp. 179. New York: McGraw-Hill 1968
13. Philpott, J.: A blade tissue study of leaves of forty-seven species of ficus. Bot. Gaz. **115**, 15–35 (1953)
14. Turing, A. M.: The chemical basis of morphogenesis. Phil. Trans. Roy. Soc. **B237**, 37–72 (1952)
15. Upadhyaya, S. K., Rand, R. H., Cooke, J. R.: A mathematical model of the effects of CO_2 on stomatal dynamics. ASAE Paper No. 80-5517. St. Joseph, Michigan: Amer. Soc. Ag. Eng. 1980
16. Saxe, H.: A structural and functional study of the coordinated reactions of individual Commelina communis L. stomata (commelinaceae). Amer. J. Bot. **66**, 1044–1052 (1979)
17. Ellenson, J.: Personal communication. Boyce Thompson Institute, Cornell University, Ithaca, NY 14853 1982
18. Nobel, P. S.: Introduction to biophysical plant physiology, pp. 488. San Francisco: Freeman 1974
19. Meidner, H., Sheriff, D. W.: Water and plants, pp. 148, New York: Wiley 1976
20. Cowan, I. R.: Oscillations in stomatal and plant functioning associated with stomatal conductance: Observations and a model. Planta (Berl) **106**, 185–219 (1972)

Received March 8/Revised April 19, 1982